ELSEVIER

Journal of Photochemistry and Photobiology A: Chemistry 108 (1997) 135–142

Journal of PHOTOCHEMISTRY AND PHOTOBIOLOGY A:CHEMISTRY

Ground and excited state prototropic behavior of 1-(purin-6-yl)-3-methylimidazolium chloride [1]

G. Wenska [a], B. Skalski [a], M. Insinska [a], S. Paszyc [a], R.E. Verrall [b]

[a] *Faculty of Chemistry, A. Mickiewicz University, Poznan, 60-780, Poland*

[b] *Department of Chemistry, University of Saskatchewan, 110 Science Crescent, Saskatoon, S7N 5C9, Saskatchewan, Canada*

Received 29 November 1996; accepted 6 February 1997

Abstract

The ground and excited state acid–base properties of the compound 1-(purin-6-yl)-3-methylimidazolium chloride, **2**, have been studied in aqueous solutions by means of UV absorption and fluorescence (steady state and time resolved) measurements. The ground state exhibits cation–zwitterion and cation–divalent cation equilibria with $pK_a = 7.25 \pm 0.05$ and -1.3 ± 0.1, respectively. Within the pH range 5.3–3, the cationic form of **2** undergoes deprotonation in the excited singlet state leading to a highly fluorescent zwitterionic species. However, the equilibrium is not established within the excited singlet state lifetime and it is estimated that only a fraction ($\approx 12\%$) of the excited molecules undergoes deprotonation. Using the Förster cycle, an excited singlet state $pK_a^* = 1.5$ is estimated from the steady state absorption and fluorescence emission spectral data. In the range $1 < pH < 3.5$, phototautomerization of the cation, leading to an excited tautomer protonated at purine nitrogen N3, occurs in addition to deprotonation. At high acidities ($pH < 1$) only the cation and the phototautomer emissions are observed. The fluorescence parameters for both the cation and phototautomer correlate well with the fluorescence data for the respective methyl analogs of the two compounds, namely 1-(9-methylpurin-6-yl)-3-methylimidazolium chloride, **3**, and 1-(3-methylpurin-6-yl)-3-methylimidazolium chloride, **4**. © 1997 Elsevier Science S.A.

Keywords: 1-(Purin-6-yl)-3-methylimidazolium chloride; UV spectroscopy; Zwitterionic; Phototantomerization; Ground state prototropic equilibria

1. Introduction

Fluorescent *N*-purinyl- and *N*-pyrimidinyl-pyridinium and -imidazolium compounds are important synthetic intermediates in the chemistry of nucleic acids [1]. Also, they have been subjected to a number of photophysical [2–7] and photochemical [8–10] studies aimed at elucidating their potential for use as fluorescent or photochemical probes in nucleic acids. Most of these studies have focused on the pyridinium compounds, in particular those derived from purine bases, whereas the respective imidazolium derivatives have received little attention, so far. Among the *N*-(purin-6-yl)-pyridinium derivatives of particular interest are those derived from tri-*O*-acetylinosine and hypoxanthine, namely *N*-[9-(2′,3′,5′-tri-*O*-acetyl-β-D-ribofuranosyl)-purin-6-yl]pyridinium chloride and *N*-(9-*H*-purin-6-yl)-pyridinium chloride, **1**. The former undergoes efficient, light induced transformation into another highly fluorescent nucleoside named tri-*O*-acetyl-luminarosine [7,8] whereas the latter appears to undergo an excited state proton transfer reaction leading to a photochemically stable zwitterionic species [2]. The ground and excited state acid–base properties of the *N*-(9-*H*-purin-6-yl)-pyridinium chloride, **1**, have been studied in detail [2]. It was shown that strong, excited state, intramolecular charge transfer interaction between the electron deficient pyridinium substituent and the purine ring leads to a drastic decrease in the pK_a, which in turn contributes to a very rapid, excited state deprotonation of **1** on a picosecond time scale.

The interesting photophysical properties of the *N*-(purin-6-yl)-pyridinium salts have prompted us to extend our studies to include the imidazolium analogs of these compounds. In this paper we report the results of UV spectroscopic as well as steady-state and time dependent fluorescence studies of the imidazolium counterpart of **1**, namely 1-(purin-6-yl)-3-methylimidazolium chloride, **2**, and its N(9)-methyl, **3**, and N(3)-methyl, **4**, derivatives in aqueous solution (Scheme 1).

[1] Preliminary results were presented at the International Symposium on Physical Organic Photochemistry, Poznan, Poland, July 1995.

PII S1010-6030(97)00076-2

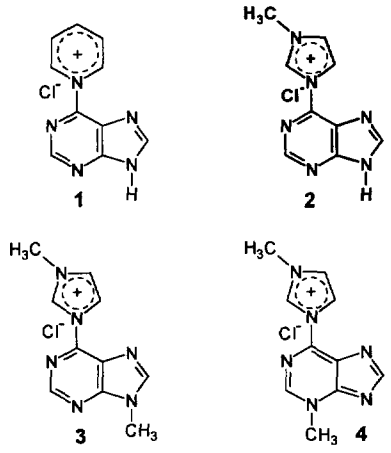

Scheme 1.

The two methyl derivatives serve as models of the two tautomeric forms of the primary compound.

2. Experimental

2.1. Materials

Analytical grade sodium hydroxide, perchloric acid, sulfuric acid and HPLC grade acetonitrile (Aldrich) were used as received. Water was purified by using a Millipore Super-Q system.

2.2. Preparation of the compounds

1-(9-methylpurin-6-yl)-3-methylimidazolium chloride, **3**, and 1-(3-methylpurin-6-yl)-3-methylimidazolium chloride, **4**, were synthesized from 9-methylhypoxanthine and 3-methylhypoxanthine [11], respectively, according to a previously described procedure [1a]. A slightly modified version of this procedure was also used for the synthesis of 1-(purin-6-yl)-3-methylimidazolium chloride, **2**. Thus, hypoxanthine (136 mg, 1 mmol) was reacted with 4-chlorophenyl-dichlorophosphate (450 mg, 1.8 mmol) in dry CH_3CN (10 ml) in the presence of 1-methylimidazole (500 mg, 6 mmol). The crude product was purified on a reversed phase silica gel (Merck) column eluted initially with water followed by a mixture of water and acetonitrile (95/5, v/v, pH ≈ 4 adjusted with $HClO_4$). Fractions containing the desired product materials were collected, concentrated and passed through a Dowex-1 (Cl^- form) column. The eluate was concentrated to dryness to give chromatographically pure **2** as a white solid (225 mg, 95% yield). The purity of the 3-methylimidazolium chlorides, (**2**, **3** and **4**) was checked by HPLC on a reversed phase Delta Pak C-4 column (Waters Millipore) eluted isocratically with 0.1 M aq. ammonium acetate containing 7.5% acetonitrile (v/v). The new compounds (**2** and **4**) exhibit correct spectral and analytical data. Included below are ^1H and ^{13}C NMR, data for **2** and **4** in D_2O.

Compound **2**; ^1H NMR (δ ppm): 10.03 (s, 1, imid 2-H), 8.38 (s, 1, pur 2-H), 8.22 and 7.64 (2 m, total 2, imid 4-H and 5-H), 8.19 (s, 1, pur 8-H), 4.07 (s, 3, methyl group). ^{13}C NMR (δ ppm): 165.94, 159.98, 148.63, 140.38, 139.54, 131.77, 125.08, 120.81, 37.33.

Compound **4**; ^1H NMR (δ ppm): 9.95 (s, 1, imid 2-H), 8.80 (s, 1, pur 2-H), 8.52 and 7.61 (2 m, total 2H, imid 4-H and 5-H), 8.41 (s, 1, pur 8-H), 4.16 and 3.94 (2 s, total 6, methyl groups). ^{13}C NMR (δ ppm): 162.69, 158.79, 144.53, 140.93, 138.13, 128.33, 125.75, 121.36, 39.27, 37.69.

2.3. Methods

Absorption spectra were recorded with a Perkin Elmer Lambda 17 UV–VIS spectrophotometer. Corrected fluorescence emission and excitation spectra were recorded using Spex Fluorog-2 and Perkin Elmer LS-50 B spectrofluorometers. Fluorescence emission from the solvents was found to be insignificant. Fluorescence quantum yields were determined using quinine sulfate in 0.1 N H_2SO_4 as a standard ($\varphi_f = 0.51$) [12]. Fluorescence lifetimes were measured using the time correlated single photon counting technique with a picosecond laser system described in detail elsewhere [13] and also with an IBH Consultants (Glasgow, Scotland) model 5000 fluorescence lifetime spectrometer using a H_2-filled nanosecond flashlamp (IBH) as an excitation source. Reconvolution of fluorescence decay curves was performed using the IBH Consultants version 4 software. The acidity of aqueous solutions used in the absorption and fluorescence measurements was varied within the range of pH 1–11 by using perchloric acid and sodium hydroxide, and the ionic strength was kept constant with sodium perchlorate (0.1 mol dm^{-3} in all of the solutions). A modified Hammett acidity scale [14] for H_2SO_4–H_2O mixtures, was used below pH 1.

3. Results and discussion

3.1. Ground state prototropic equilibria for compounds 2–4 in aqueous solution

The pH dependence of the UV absorption spectra of compound **2** is shown in Fig. 1. In acidic solutions ($1.0 < pH < 5.5$) the spectrum consists of a single band in the 236–310 nm wavelength range centered at 279 nm with a shoulder on the short wavelength side. The similarity of this spectrum with that of the N9-methyl substituted chromophore **3** (see Table 1) indicates that, within this pH range, the ground state of **2** is dominated by the cationic form with a proton attached to N(9) of the purine ring (Scheme 1), i.e. the tautomeric form characteristic of the parent purine molecule [15]. One should note that purine tautomers with a proton attached to the pyrimidine part (i.e. N3-H or N1-H tautomers) exhibit UV characteristics different from that for the tautomers with H attached to the imidazole part of the purine ring [15]. The ground state tautomeric homogeneity

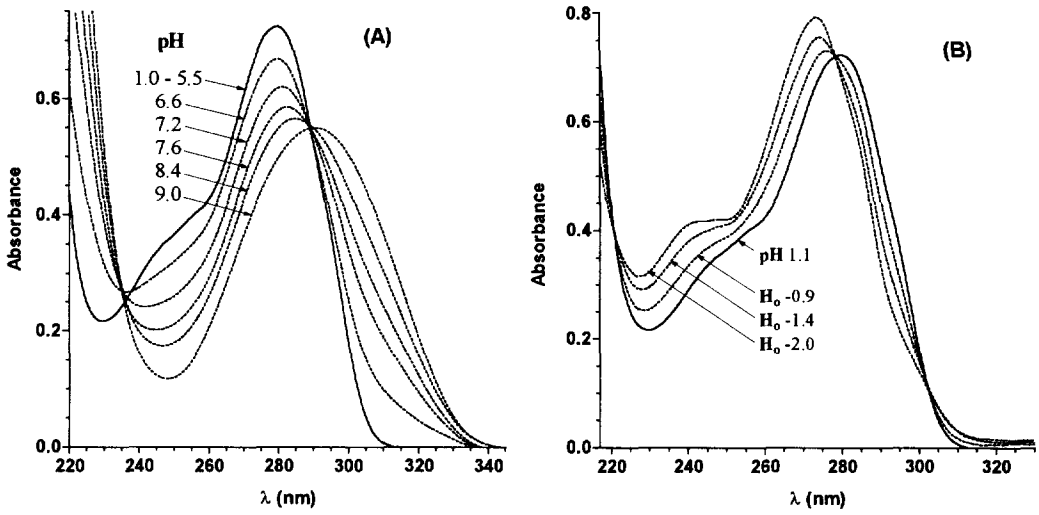

Fig. 1. The pH dependence of the absorption spectra of 1-(purin-6-yl)-3-methylimidazolium chloride, **2**, in water.

Table 1
UV absorption and fluorescence data for the prototropic species of the 1-(purin-6-yl)-3-methylimidazolium chloride, **2** and compounds **3** and **4**

Compound	Solvent	Absorption			Fluorescence			
		Dominant species	λ_{max} (nm)	(ϵ) ($l\,mol^{-1}\,cm^{-1}$)	Dominant species	λ_{max} (nm)	φ	τ (ns)
2	water pH 9.5	zwitterion	–	291 (8600)	zwitterion	390	0.75	8.85
	water pH 5.3	cation	248 (sh, 5200)	279 (10900)	zwitterion	390		
					cation	344		0.085
	water pH 0.5	cation	248 (sh, 5200)	279 (10900)	cation	344		
					phototautomer	410		8.22
2	CH_3CN	cation	255 (sh, 5300)	281 (11500)	cation	350	0.002	0.10
3	water pH 1–9.5	cation	248 (sh, 5100)	278 (9800)	cation	345	0.036	0.25
4	water pH 3–9.5	cation	–	290 (8200)	cation	411	0.227	8.14

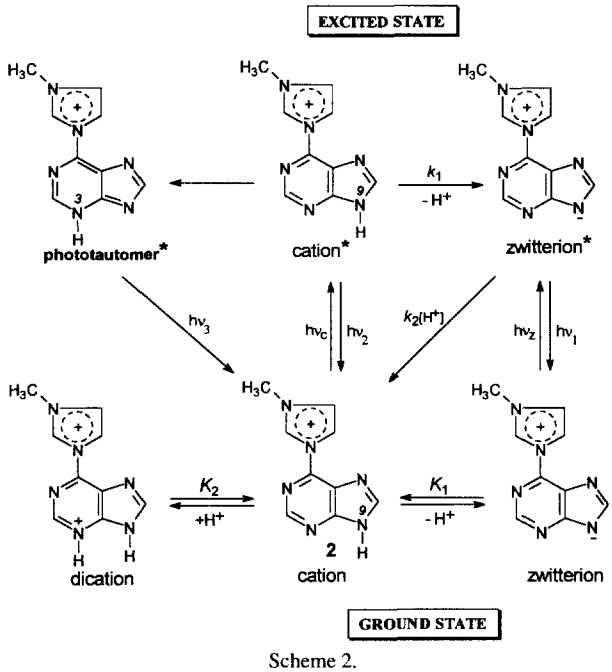

Scheme 2.

of **2** in this pH range is further supported by the lack of an emission wavelength dependence of the corresponding fluorescence excitation spectra which also coincide well with the absorption spectrum.

Increasing the pH of an aqueous solution of **2** to ca. 9.5 results in a gradual decrease in the intensity of the 279 nm band with the concomitant appearance of a new absorption band with a maximum at $\lambda = 291$ nm and a clear isosbestic point at 288 nm (cf. Fig. 1(A) and Table 1). The observed changes in the UV spectrum of **2** within this pH range can be attributed to a ground state cation–zwitterion equilibrium presented in Scheme 2. The estimated value of $pK_a = 7.25$ for this equilibrium is obtained from the corresponding spectrophotometric titration curve shown in Fig. 6. As would be expected, due to the presence of an electron withdrawing, imidazolium substituent in **2**, this pK_a value is much smaller than that for an unsubstituted purine ring ($pK_a = 8.93$) [15]. On the other hand, it is a half unit greater than that found for *N*-(purin-6-yl)-pyridinium chloride, **1**, ($pK_a = 6.7$) [2] which possesses a stronger electron accepting pyridinium group as a substituent.

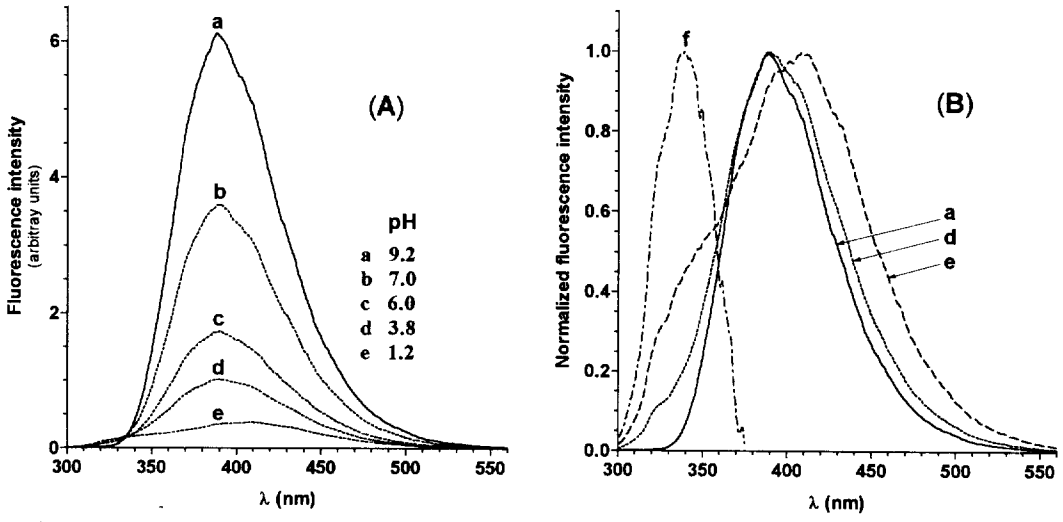

Fig. 2. (A) The pH dependence of the fluorescence spectra of 1-(purin-6-yl)-3-methylimidazolium chloride, **2**, in water, and (B) selected fluorescence spectra from part (A), after normalization, and the normalized spectrum of the cationic form of **2** (spectrum **f**) obtained as described in the text (Section 3.3). Excitation wavelength is 288 nm.

The absorption spectrum of **1** undergoes further changes when the aqueous solution becomes strongly acidic (pH < 1, cf. Fig. 1(B)). These changes can be attributed to the protonation of **2** which leads to the formation of a divalent cation (Scheme 2). The value of $pK_a = -1.3 \pm 0.1$ is obtained for the cation–dication equilibrium from the spectrophotometric measurements.

The UV absorption spectra of the methyl derivatives **3** and **4** (Table 1) are independent of pH except at high acid concentrations, where protonation occurs. The spectral changes observed under these conditions (spectra not shown) are similar to these accompanying divalent cation formation in the case of compound **2**, i.e. the long wavelength absorption band shifts to the blue and its intensity increases slightly. The corresponding ground state cation–divalent cation equilibria for compounds **3** and **4** have values of $pK = -1.6 \pm 0.1$ and 1.0 ± 0.05, respectively.

As would be expected, in dry acetonitrile solution where no proton transfer occurs, the UV absorption spectrum of **2** is similar to that in water at pH range 5.5–1.0, corresponding to the protonated cationic form (see Table 1).

3.2. Steady-state and time-resolved fluorescence studies

The pH dependence of the fluorescence spectra of compound **2** is shown in Fig. 2. In basic solution (pH = 9.5), where the zwitterionic form of **2** is practically the only ground state species present (see Scheme 1), a single fluorescence band with a maximum at $\lambda = 390$ nm and a lifetime of $\tau_1 = 8.8$ ns (cf. Figs. 2 and 3) is observed. The corresponding excitation spectrum (not shown) coincides with the absorption spectrum of the zwitterion.

As the pH is decreased, the fluorescence at 390 nm decreases gradually with a concomitant appearance of a new, weak emission located on the blue shoulder of the spectrum (Fig. 2). In agreement with this observation, starting at ca. pH 7.0 the fluorescence decay becomes nonexponential and down to ca. pH 4.0 a second, short lived component ($\tau_2 \approx 150$ ps) is needed, in addition to the long-lived component ($\tau_1 \approx 8.8$ ns), to fit the experimental decay curves reasonably well (Figs. 3 and 4). The contribution of the short-lived component to the overall decay increases dramatically at shorter wavelengths, amounting to in excess of 85% at $\lambda_{em} \leq 330$ nm, whereas there is a corresponding decrease in the long-lived component. The lifetime of 150 ps for the second component was obtained from the analysis of the decay curves recorded with a time base of 54.42 ps per channel, suitable for the longer lived component. To obtain

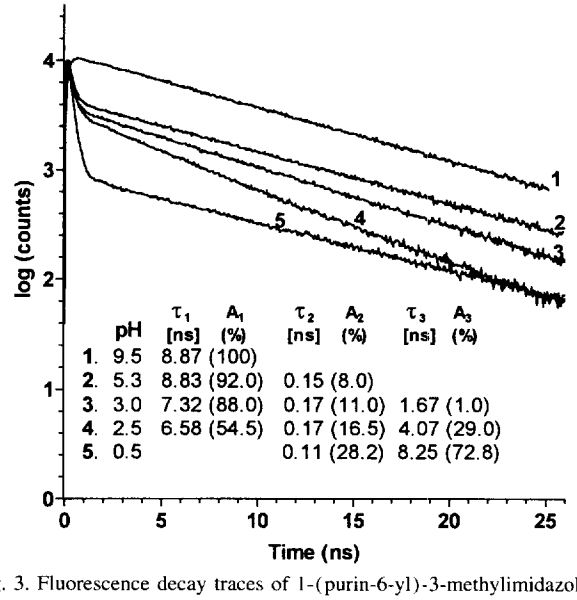

Fig. 3. Fluorescence decay traces of 1-(purin-6-yl)-3-methylimidazolium chloride, **2**, in aqueous solutions of various pH. Samples were excited at 288 nm and emission monitored at 380 nm. Included within the figure are the best fit parameters for each of the decay curves (randomly scattered weighted residuals between experimental and fitted decay curves as well as $\chi^2 \approx 1.0$–1.1 were obtained throughout).

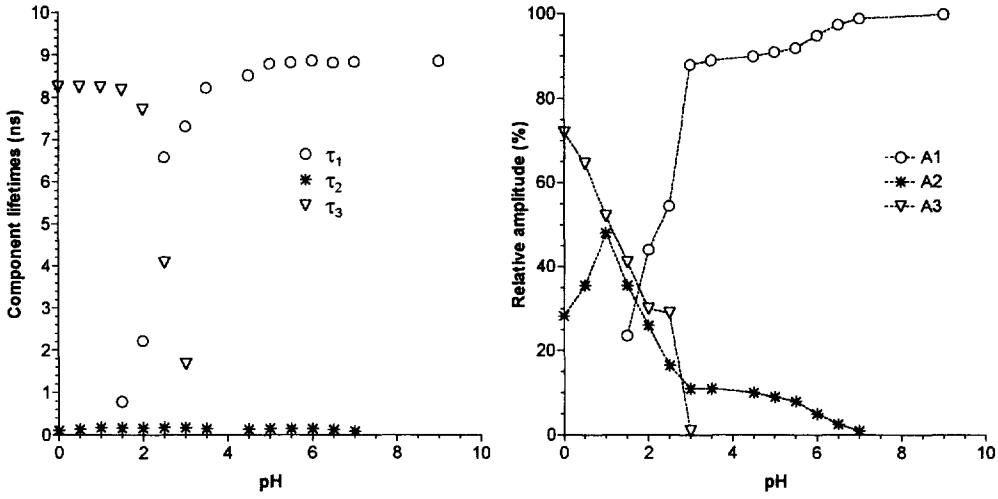

Fig. 4. The pH dependence of fluorescence component lifetimes and corresponding relative amplitudes for 1-(purin-6-yl)-3-methylimidazolium chloride, **2**, in water, derived from reconvolution analysis of experimental fluorescence decay curves.

a more precise estimate of the short component, the time base of the single-photon counting system was set to ca. 2.78 ps per channel and a series of decay curves recorded at $\lambda_{em} = 330$ nm were analyzed. A lifetime of 85 ± 5 ps was obtained for the blue emitting species within the pH range 6.5–3.0.

At higher acidities (pH range 4.0–1.5) the fluorescence intensity of the blue emitting component remains practically unchanged, whereas the component at 390 nm decreases further and eventually disappears at pH < 1.5. This is accompanied by the formation of a third, red shifted emission with a maximum around 410 nm (cf. Fig. 2(B)). The observed changes in the emission spectra correlate well with the corresponding changes in the measured lifetimes. As seen in Fig. 4, upon changing pH from 4 to 1.5 the component with a 8.8 ns lifetime, attributed to the species having a maximum emission at 390 nm, is gradually quenched and vanishes completely at pH ≈ 1.5. Simultaneously, a third component appears whose lifetime increases gradually and reaches a maximum ($\tau_3 \approx 8.2$ ns) around pH 1.5. The triexponential character of the decay curve is particularly pronounced at ca. pH 2.5 (cf. Figs. 3 and 4). The relative amplitude of the third component increases with increasing emission wavelength, in agreement with the observed red shift of the emission maximum. At pH < 1.5 only the blue and the red shifted emissions are present in the spectra excited at 288 nm and the decay curves become biexponential again.

3.3. Interpretation of the fluorescence spectra and lifetimes

Based on the ground state acid–base properties of **2**, the fluorescence at pH 9.5 ($\lambda_{max} = 390$ nm, $\tau_1 = 8.8$ ns) is assigned to the zwitterion present as the only ground state form of **2** in solution ($pK_a(S_0) = 7.25$). The blue shifted, short-lived emission appearing in the spectra at pH < 7.0 can be attributed to the cationic form of **2**, formed as a result of the ground state protonation of the zwitterion (Scheme 2). The fluorescence spectrum of the pure cationic form can not be obtained directly, as it overlaps with other intense emission(s) over the entire acidic rage (0 < pH < 7.0) studied (cf. Fig. 2). However, a reasonable approximation of such a spectrum can be obtained by subtracting the spectrum of the zwitterion alone (at pH 9.5) from that containing both the zwitterion and the cation emissions (at pH 4–5), after suitable normalization. A single band with a maximum at ≈ 340 nm is obtained (spectrum **f** in Fig. 2(B)). In support of the above assignment, a similar fluorescence spectrum ($\lambda_{max} = 344$ nm) with a subnanosecond lifetime ($\tau_f = 230$ ps) (cf. Table 1), both spectral parameters being independent of solution pH within the range 0.5–9.5, was obtained for the 9-methyl derivative **3**. This compound was synthesized as the model species of the cationic form of compound **2**.

Since in the pH range 5.0–1.0 the ground state prototropic equilibrium of **2** is shifted completely towards the cationic form, it may be concluded that both the zwitterion fluorescence (390 nm), which still dominates the overall emission of **2** within the pH range 5.0–3.0, as well as the third emission appearing at pH < 3.0 ($\lambda_{max} = 410$ nm) must originate from the species formed from the same precursor, i.e. the excited cation. Thus, the 390 nm emission can be assigned to the excited zwitterion formed from the excited cation due to an adiabatic proton transfer reaction, a process similar to that reported previously for **1** [2]. On the other hand, the 410 nm emission is assumed to originate from an excited tautomer with a proton attached to purine nitrogen N3 (cf. Scheme 2), formed as a result of the phototautomerization of the excited cation.

To check the latter assumption, 1-(3-methylpurin-6-yl)-3-methylimidazolium chloride, **4**, was synthesized as a suitable, non-tautomerizable analog of the proposed phototautomer, and its photophysical properties were determined. The relevant spectroscopic data are summarized in Table 1. Both the shape and position of the fluorescence spectrum as well as the fluorescence lifetime of **4** are independent of pH

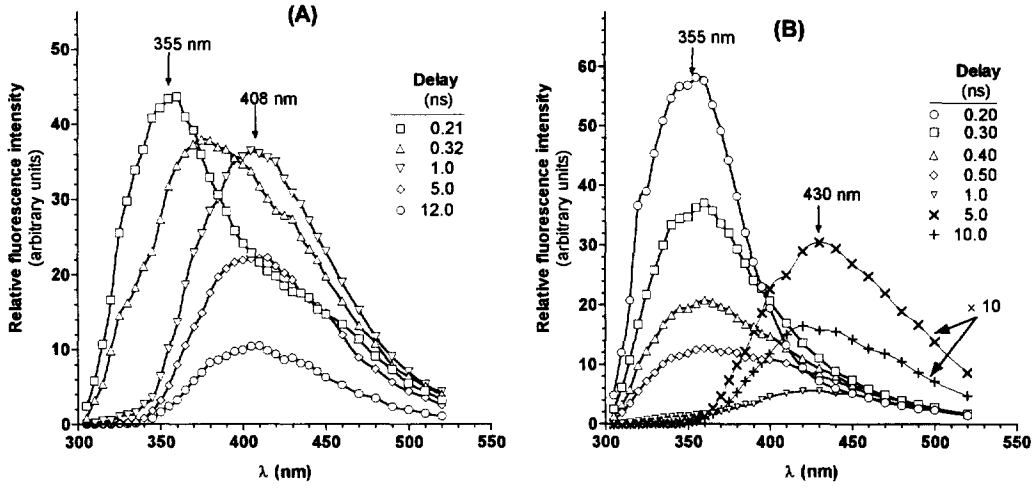

Fig. 5. Time resolved fluorescence spectra for compound **2**.

except for highly acidic solutions ($H_0 < 0$) when the intensity of the emission decreases without any changes in the band shape. As can be seen, both the fluorescence maximum (411 nm) and the lifetime (8.25 ns) of the model compound **4** are nearly identical with those of the third emitting species observed at pH < 3. This supports the proposed excited state phototautomerization of **2** at higher acidities.

A similar type of N(H)–N → N–N(H) phototautomerism has been observed in related nitrogen heterocycles including lumichromes [16], alloxazines [17], lumazine [18], complexes of 7-azaindole with alcohol [19], and the alkaloids harmaline, harmalol [20] and formycin [21].

Both the excited state proton transfer reaction as well as the phototautomerization of the excited cationic form of **2**, leading to the excited zwitterion and the 3-H phototautomer, respectively, can be observed by means of time resolved emission spectra (TRES). Using a known procedure [22], two sets of picosecond TRES, corresponding to pH 5.0 (Fig. 5(A)) and pH 1.5 (Fig. 5(B)), were generated from corresponding decay curves obtained at 5 nm wavelength intervals over the spectral range of 300–520 nm. As can be seen, a blue shifted fluorescence with a maximum at ca. 355 nm (uncorrected) dominates the fluorescence spectra obtained at short delay times (≈ 200 ps) in both cases. Both the position of this fluorescence as well as its fast decay, the intensity falls to zero within 1 ns in each case, are characteristic of the cationic form of **2**. The decrease in the intensity of the fast fluorescence at pH 5.0 is accompanied by the simultaneous appearance of the long-lived, red shifted emission of the zwitterion with a maximum at ≈ 410 nm (uncorrected) (Fig. 5(A)). Analogously, at pH 1.5 a long-decaying, red-shifted emission with a maximum around 430 nm (uncorrected), characteristic of the phototautomer, appears in the spectra as that of the cation disappears with an increasing delay time (Fig. 5(B)).

3.4. Excited state equilibria of 2

As shown in Fig. 6, the plot of the relative fluorescence intensity (F/F_0) at λ = 390 nm, characteristic of the zwitterionic form of **2**, vs. pH (F_0 refers to the fluorescence intensity of the "pure" zwitterionic form measured at pH > 9.0, i.e. in the absence of any excited state reaction) closely follows the corresponding spectrophotometric titration curve up to pH ca.7.0. It then reaches a plateau at pH 5.3 corresponding to ca. 12% of the initial value. The right hand inflection of the sigmoidal plot is situated precisely at pH 7.2, corresponding to the ground state pK, indicating that the observed intensity changes occur mainly as a consequence of the ground state cation–zwitterion equilibrium (Scheme 2). The position of the plateau at pH 5.3, where no ground state zwitterion is present, indicates that only ≈ 12% of the cationic species undergoes deprotonation within its excited state lifetime.

Such behavior resembles that found for the β-naphthoate anion and represents the general situation in which the excited state equilibrium is not established within the excited state lifetime [23–25]. Because of this fact, as well as the coexistence of excited state proton transfer and phototautomerization at higher acidities, the left hand inflection of the

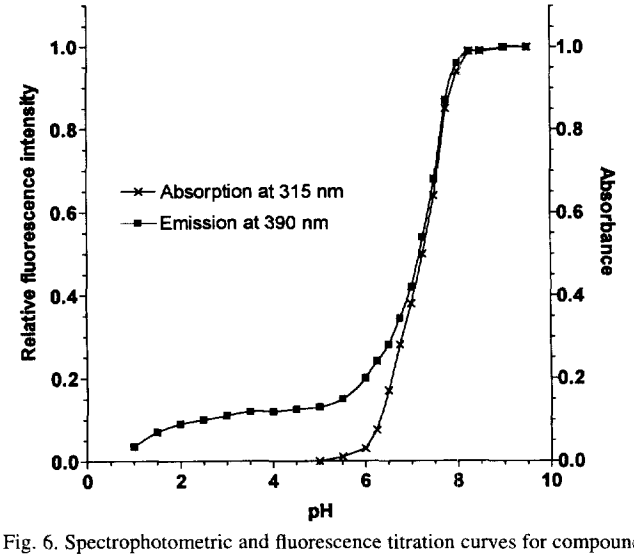

Fig. 6. Spectrophotometric and fluorescence titration curves for compound **2** plotted as the absorbance at λ = 315 nm and relative fluorescence intensity at λ = 390 nm, respectively, vs. pH.

fluorescence titration curve observed at about pH 1.5 can not be taken as a true excited singlet state pK_a^* value.

Bearing in mind, that the thermodynamic Förster cycle [26,27] gives the precise values only in special cases, we nevertheless used the equation:

$$pK_a - pK_a^* = \frac{hc(\nu_a^{AH^+} - \nu_a^{A^\pm} + \nu_f^{AH^+} - \nu_f^{A^\pm})}{2(2.303kT)}$$

where ν_a and ν_f denote the positions in cm^{-1} of the pertinent absorption and fluorescence band maxima, to obtain an approximate value of the excited pK_a^*. It is believed [23], even when the required conditions are not fulfilled, that the Förster method can give a good approximation of the magnitude of the pK_a change upon excitation. Using the appropriate experimental data presented in Table 1, a value of $pK_a^* = 1.5$ is obtained.

The excited state pK_a^* can also be estimated by considering the rates of the forward and the back proton transfer reactions (see Scheme 2). The rate constant k_1 for deprotonation of the cation can be calculated using the relation $k_1 = 1/\tau - 1/\tau_0$, where τ_0 and τ represent the lifetimes of the cation in the absence and in the presence of the excited state reaction, respectively [24,25]. Since τ_0 could not be determined directly in aqueous solution, a lifetime for **2** in acetonitrile (Table 1), where no excited state deprotonation occurs, was used. Based on this assumption, a value of $k_1 = 2 \times 10^9\ s^{-1}$ is obtained. This value is an order of magnitude smaller than that found for deprotonation of excited *N*-(purin-6-yl)pyridinium cation, **1**, [2] but still higher than that reported for 2-naphtol ($k = 1.0 \times 10^8\ s^{-1}$) [28]. The back reaction rate constant k_2 can be estimated from the lifetime data for the zwitterion at higher acidities (pH 4–1). As seen in Fig. 4, the lifetime of the zwitterion decreases with acidity at pH < 4 and the plot of τ_0/τ versus $[H^+]$ (not shown) is linear, as would be expected for dynamic quenching of the zwitterion by protons. Fitting a straight line to this plot yielded the value of $k_2 = 3.3 \times 10^{10}\ dm^3\ mol^{-1}\ s^{-1}$ for the protonation of the zwitterion. As would be expected for such a process, this value is very close to the diffusion-controlled limit ($5 \times 10^{10}\ dm^3\ mol^{-1}\ s^{-1}$) [29]. Using the estimated values of k_1 and k_2, a value of $pK^* = -\log(k_1/k_2) = 1.22$, in good agreement with that obtained from the Förster cycle, is obtained.

Finally, the extent of the phototautomerization process requires further comment. The degree to which this process occurs is difficult to estimate since the fluorescence quantum yield of the N3-H tautomer cannot be measured directly. However, an estimate can be made by assuming that at pH 1.0, the condition at which the lifetime of the tautomer reaches its maximum value ($\tau_3 = 8.25$ ns, cf. Fig. 4), its quantum yield is close to that of the N3-methyl derivative, **4** (see Table 1). Thus, resolving the fluorescence spectrum at pH 1.0 into the component emissions of the cation and the phototautomer and comparing the latter with that of the zwitterion alone (at pH 9.0) indicates that at least 26% of the

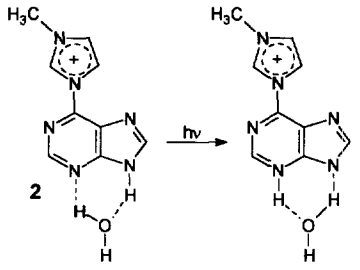

Scheme 3.

cation (the only ground state species present in a solution at pH 1.0) undergoes phototautomerization.

The fact that phototautomerization of **2** could not be observed in dry acetonitrile indicates the involvement of water in this process. Two parallel tautomerization processes can be considered: (i) protonation of the excited cation at purine nitrogen N3 followed by deprotonation at N9, and (ii) a one step reaction in which one water molecule, interacting with the cation via hydrogen bonding, could allow for the simultaneous deprotonation of purine nitrogen N9 and protonation of nitrogen N3 (Scheme 3). Taking into account the very short lifetime of the excited cation and the relatively low concentration of protons in the pH range 3–1, the first possibility can be practically ruled out. Thus, it is assumed that within the range of pH 3–1 mechanism (ii) operates. At pH < 1, when the ground state cation–dication equilibrium exists, tautomerization via deprotonation of the excited dication should also be considered (Scheme 2) in addition to the concerted process (ii).

Both the steady state and time resolved fluorescence data clearly indicate that the excited state acidity constant (pK_a^*) for purine nitrogen N3 of the phototautomer must be slightly higher than that for deprotonation of the cation at N9 site ($pK_a^* \approx 1.5$). However, for reasons similar to those advanced in the case of the deprotonation of the cation (see above), the exact value of pK_a^* can not be obtained. Based on the pH dependence of the component lifetimes shown in Fig. 4, an optimal range of 2–2.5 for this value can be predicted.

It is interesting to note that an analogous phototautomerization process was not observed in the case of the pyridinium compound **1** [2]. This difference in behavior between the two, although structurally, closely related compounds, may be due to the stronger electron withdrawing effect of the pyridinium substituent in the case of **1**, resulting in a much higher acidity of purine nitrogen N3.

4. Conclusion

Photophysical studies of the 1-(purin-6-yl)-3-methylimidazolium chloride, **2**, in aqueous solutions over a wide pH range have enabled the determination of its acid–base properties in the ground and excited states. UV absorption measurements indicate the occurrence of ground state cation–

zwitterion and cation–dication prototropic equilibria for **2** with pK_a values of 7.25 and −1.3, respectively.

Upon excitation the purine ring nitrogen N9 in **2** becomes more acidic resulting in deprotonation of the cation, however, the proton transfer equilibrium is not established within the excited state lifetime It is estimated that only a fraction (ca. 12%) of the excited cation undergoes deprotonation within the pH range 5–3. The corresponding excited state acidity constant $pK_a^* \approx 1.5$ is estimated from a Förster cycle calculation.

At pH < 3 phototautomerization of the cation occurs in addition to deprotonation. The UV absorption and fluorescence spectral data of the phototautomer are nearly identical with those of the 3-methyl derivative **4** indicating that a tautomeric species with a proton attached to purine nitrogen N3 is formed upon phototautomerization of the cation.

Acknowledgements

Partial financial support from the Polish Research Committee (within the project PN 1031/92/02) is gratefully acknowledged. REV acknowledges the financial support of the Natural Sciences and Engineering Research Council of Canada.

References

[1] (a) R.W. Adamiak, E. Biala, B. Skalski, Nucleic Acids Res. 13 (1985) 2989; (b) R.W. Adamiak, E. Biala, B. Skalski, Angew. Chem. Int. Ed. Engl. 24 (1985) 12; (c) R.W. Adamiak, E. Biala, Z. Gdaniec, S. Mielewczyk, B. Skalski, Chem. Scr. 26 (1986) 3; (d) R. Fathi, B. Goswami, P.-P. Kung, B.L. Gaffney, R.A. Jones, Tetrahedron Lett. 31 (1990) 319; (e) G. Wenska, B. Skalski, Z. Gdaniec, Can. J. Chem. 70 (1992) 856; (f) H. Gao, R. Fathi, B.L. Gaffney, B. Goswami, P.-P. Kung, Y. Rhee, R. Jin, R.A. Jones, J. Org. Chem. 57 (1992) 6954; (g) A. Burdzy, B. Skalski, E. Biala, R.W. Adamiak, Nucleosides and Nucleotides 14 (1995) 979.

[2] B. Skalski, R.P. Steer, R.E. Verrall, J. Am. Chem. Soc. 110 (1988) 2055.

[3] B. Skalski, S. Paszyc, R.W. Adamiak, R.P. Steer, R.E. Verrall, Can. J. Chem. 68 (1990) 2164.

[4] G. Wenska, B. Skalski, S. Paszyc, S. Wnuk, R.W. Adamiak, J. Fluoresc. 4 (1994) 283.

[5] G. Wenska, B. Skalski, S. Paszyc, J. Photochem. Photobiol. A: Chem. 57 (1991) 279.

[6] G. Wenska, B. Skalski, J. Koput, S. Paszyc, J. Photochem. Photobiol. A: Chem. 88 (1995) 117.

[7] B. Skalski, S. Paszyc, R.W. Adamiak, R.P. Steer, R.E. Verrall, J. Chem. Soc. Perkin Trans. II, (1989) 1691.

[8] B. Skalski, J. Bartoszewicz, S. Paszyc, Z. Gdaniec, R.W. Adamiak, Tetrahedron 43 (1987) 3955.

[9] B. Skalski, R.P. Steer, R.E. Verrall, J. Am. Chem. Soc. 113 (1991) 1756.

[10] G. Wenska, B. Skalski, S. Paszyc, Can. J. Chem. 73 (1995) 2178.

[11] J.W. Jones, R.K. Robins, J. Am. Chem. Soc. 84 (1962) 1914.

[12] A. Eaton, Pure Appl. Chem. 60 (1988) 1107.

[13] W. Augustyniak, J. Koput, A. Maciejewski, M. Sikorski, R.P. Steer, M. Szymanski, Pol. J. Chem. 67 (1993) 1409.

[14] A. Albert, E.P. Serjeant, in: The Determination of Ionization Constants, Chapman and Hall, New York, 1984, p. 70ff.

[15] G. Shaw, in: A.R. Katritzky, C.W. Reesm (Eds.), Comprehensive Heterocyclic Chemistry, vol. 5, Pergamon, New York, 1984, p. 499ff.

[16] R.D. Fugate, P.-S. Song, Photochem. Photobiol. 24 (1976) 479.

[17] P.-S. Song, M. Sum, A. Koziolowa, J. Koziol, J. Am. Chem. Soc. 96 (1974) 4319.

[18] R. Klein, I. Tatischeff, Photochem. Photobiol. 45 (1987) 55.

[19] K.C. Inham, M.A. El-Bayoumi, J. Am. Chem. Soc. 96 (1974) 1674.

[20] M. Krishnamurthy, S.K. Dogra, Photochem. Photobiol. 44 (1986) 571.

[21] K.L. Wierzchowski, D. Shugar, Photochem. Photobiol. 35 (1982) 445.

[22] J.M. Easter, R.P. DeToma, L. Brand, Biophys. J. 16 (1976) 571.

[23] J.F. Ireland, P.A.H. Wyatt, Adv. Phys. Org. Chem. 12 (1976) 131ff.

[24] J.R. Lakowicz, in: Principles of Fluorescence Spectroscopy, Plenum, New York, 1983, p. 383.

[25] J.B. Birks, Nouv. J. Chem. 1 (1977) 453.

[26] A. Weller, Prog. React. Kinet 1, (1961) 189.

[27] E. Vander Donckt, Prog. React. Kinet 5, (1970) 273.

[28] L.G. Arnaut, S.J. Formoshino, J. Photochem. Photobiol. A: Chem. 75 (1993) 1.

[29] M. Eigen, Angew. Chem., Int. Ed. Engl. 3 (1964) 1.